

Opportunities for Probing $U(1)_{T3R}$ with Light Mediators

Bhaskar Dutta^{*1}, Sumit Ghosh^{†1}, and Jason Kumar^{‡2}

¹*Mitchell Institute for Fundamental Physics and Astronomy, Department of Physics and Astronomy,
Texas A&M University, College Station, Texas 77843-4242, USA*

²*Department of Physics and Astronomy, University of Hawaii, Honolulu, Hawaii 96822, USA*

We consider strategies for using new datasets to probe scenarios in which light right-handed SM fermions couple to a new gauge group, $U(1)_{T3R}$. This scenario provides a natural explanation for the light flavor sector scale, and a motivation for sub-GeV dark matter. There is parameter space which is currently allowed, but we find that much of it can be probed with future experiments. In particular, cosmological and astrophysical observations, neutrino experiments and experiments which search for displaced visible decay or invisible decay can all play a role. Still, there is a small region of parameter space which even these upcoming experiments will not be able to probe. This model can explain the observed $2.4\text{--}3\sigma$ excess of events at the COHERENT experiment in the parameter space allowed by current laboratory experiments, but the ongoing/upcoming laboratory experiments will decisively probe this possibility.

I Introduction

A well-motivated scenario for new physics beyond the Standard Model (BSM) is the existence of new gauge groups. One well-studied gauge group, first considered in the context of left-right-models [1, 2, 3], is $U(1)_{T3R}$. In this scenario, a set of right-handed Standard Model (SM) fermions are charged under the new gauge group, while left-handed SM fermions remain uncharged. It was recently pointed out [4] that, if there is a low symmetry-breaking scale, then this scenario naturally lead to sub-GeV dark matter because the dark sector mass scale is tied to that of the light SM fermions.

There are a variety of experimental and observational bounds on this scenario, but there is still open parameter space which evades all current constraints, and in which the dark matter candidate can achieve the correct relic density. In this work, we will consider prospects for future datasets to definitively probe the entirety of the open parameter space.

In this scenario, some right-handed first- and/or second-generation fermions are charged under $U(1)_{T3R}$, and this symmetry protects their masses. If the symmetry-breaking scale is $\lesssim \mathcal{O}(10)$ GeV, then these SM fermions naturally obtain sub-GeV masses. Moreover, this symmetry-breaking scale can naturally feed into the dark sector, yielding sub-GeV dark matter which interacts with the Standard Model through the processes mediated by a low-mass dark photon (A') or dark Higgs (ϕ').

We will find that, under certain assumptions, this scenario can be tightly constrained by cosmological and astrophysical observations. Collider, fixed-target, beam-dump, and coherent elastic neutrino-nucleus scattering (CE ν NS) experiments can produce large fluxes of the dark photon and dark Higgs, which can be effectively probed by searching either for visible decays at distant detectors, or evidence for invisible decays. Invisible decays of the dark photon and dark Higgs can also produce a flux of either sterile neutrinos or of dark matter, which can be searched for at distant detectors which look for scattering. We will see that models in the allowed parameter space can explain the COHERENT excess, which is associated with dark matter/sterile neutrinos emerging from the decays of the dark photon [5]. Finally, this scenario can also produce non-standard interactions (NSI) of active neutrinos, mediated by the A' or ϕ' , which are being probed in various types of neutrino experiments.

These new searches can potentially rule out or find evidence for models in much of the allowed parameter space. But there are still regions of the parameter space which will evade bounds from upcoming experiments; for these models, the mediators decay rapidly into SM particles, leaving no signals at displaced detectors and signals at nearby detectors which are difficult to distinguish from background.

The outline of this paper is as follows. In Sec. II, we describe the model, and the interactions of the dark photon and dark Higgs. In Sec. III, we describe constraints arising from cosmological and astrophysical observables. In Sec. IV, we describe constraints arising from visible decays at displaced detectors. We describe

^{*}dutta@physics.tamu.edu

[†]ghosh@tamu.edu

[‡]jkumar@hawaii.edu

constraints arising from decays at nearby detectors in Sec. V. In Sec. VI, we describe constraints on dark matter or sterile neutrino scattering at detectors displaced from a beam source. In Sec. VII, we describe constraints on non-standard active neutrino interactions. We conclude with a discussion of our results including a summary table in Sec. VIII.

II Model

The details of this scenario are described in Ref. [4], but we briefly review the relevant properties here. A set of right-handed Standard Model fermions are charged under $U(1)_{T3R}$, with up-type fermions having charge +2 and down-type fermions having charge -2. If a full generation of right-handed SM fermions (including a right-handed neutrino) are charged under $U(1)_{T3R}$, then all gauge and gravitational anomalies cancel. The gauge boson of $U(1)_{T3R}$ is the dark photon, A' , with gauge coupling g_{T3R} .

We assume that the fermions charged under $U(1)_{T3R}$ are first- or second-generation, with sub-GeV masses. Note that, to cancel anomalies, it is necessary for a right-handed up-type quark, down-type quark, charged lepton and neutrino to be charged under $U(1)_{T3R}$, but they need not all be in the same generation. As shown in [6], it is technically natural for one quark (the up-type quark, for example) and the charged lepton to be mass eigenstates. But if second-generation quarks are charged under $U(1)_{T3R}$, then there are tight constraints arising from measurements of anomalous Kaon decay. We will therefore assume that the right-handed u - and d -quarks are charged under $U(1)_{T3R}$. We will also see that there are tight bounds on the scenario where electrons are charged under $U(1)_{T3R}$, arising from cosmological observables [7] and atomic parity violation experiments [8]. We will therefore assume that the right-handed muon is charged under $U(1)_{T3R}$. We also add a left-handed and right-handed fermion pair η_L and η_R , which are SM singlets, but are charged under $U(1)_{T3R}$ with charges ± 1 . The $U(1)_{T3R}$ charge assignments are summarized in Table. 1

Table 1: The charges of the fields which transform under $U(1)_{T3R}$. For the fermionic fields, the shown charges are for the left-handed component of each Weyl spinor.

field	u_R	d_R	μ_R	ν_R	η_L	η_R	ϕ
q_{T3R}	-2	2	2	-2	1	-1	2

With the given field content, the interaction Lagrangian can be written as,

$$\begin{aligned} \mathcal{L} = & - \frac{\lambda_u}{\Lambda} \tilde{H} \phi^* \bar{Q}_L u_R - \frac{\lambda_d}{\Lambda} H \phi \bar{Q}_L d_R - \frac{\lambda_\nu}{\Lambda} \tilde{H} \phi^* \bar{L}_L \nu_R - \frac{\lambda_\mu}{\Lambda} H \phi \bar{L}_L \mu_R - m_D \bar{\eta}_R \eta_L - \frac{1}{2} \lambda_L \phi \bar{\eta}_L^c \eta_L \\ & - \frac{1}{2} \lambda_R \phi^* \bar{\eta}_R^c \eta_R - \mu_\phi^2 \phi^* \phi - \lambda_\phi (\phi^* \phi)^2 + H.c., \end{aligned} \quad (1)$$

where Q_L and L_L denote the left-handed SM quark and lepton doublet, respectively; H is the SM Higgs doublet; and \tilde{H} is defined as $\tilde{H} = i\tau_2 H^*$.

$U(1)_{T3R}$ is broken by the condensation of a field ϕ , which has charge +2. This breaks $U(1)_{T3R}$ down to a parity, under which SM fermions are even. We can then express this field as $\phi = V + \phi'/\sqrt{2}$, where V is the vacuum expectation value of ϕ , and ϕ' is the dark Higgs with mass $m_{\phi'} = 2\lambda_\phi^{1/2} V$. The mass matrix for η contains both Dirac terms, m_D , and Majorana terms, m_M , the latter of which are necessarily proportional to V as $m_M = \lambda_M V$, where we assume that $\lambda_L = \lambda_R$. We assume that the Dirac terms are small compared to the Majorana terms, leaving us with two Majorana fermions, η_1 and η_2 , with masses $m_1 = m_M - m_D$ and $m_2 = m_M + m_D$ respectively. The mass splitting is very small, $\Delta m = 2m_D$. The $\eta_{1,2}$ are odd under the surviving parity, and the lighter one, η_1 is a dark matter candidate. In the low-energy effective field theory below the electroweak symmetry-breaking scale, SM fermions have Yukawa coupling terms and mass terms of the form

$$\begin{aligned} \mathcal{L} = & - m_u \bar{u}_L u_R - m_d \bar{d}_L d_R - m_{\nu D} \bar{\nu}_L \nu_R - m_\mu \bar{\mu}_L \mu_R - \frac{1}{2} m_1 \bar{\eta}_1 \eta_1 - \frac{1}{2} m_2 \bar{\eta}_2 \eta_2 - \frac{m_u}{V\sqrt{2}} \bar{u}_L u_R \phi' \\ & - \frac{m_d}{V\sqrt{2}} \bar{d}_L d_R \phi' - \frac{m_{\nu D}}{V\sqrt{2}} \bar{\nu}_L \nu_R \phi' - \frac{m_\mu}{V\sqrt{2}} \bar{\mu}_L \mu_R \phi' - \frac{1}{2\sqrt{2}} \frac{m_1}{V} \bar{\eta}_1 \eta_1 \phi' - \frac{1}{2\sqrt{2}} \frac{m_2}{V} \bar{\eta}_2 \eta_2 \phi' + H.c., \end{aligned} \quad (2)$$

The mass matrix for $\nu_{L,R}$ contains a Dirac mass term, $m_{\nu D}$, which is proportional to V , and can contain a Majorana mass for ν_R which scales as $\propto V^2/\Lambda$, where Λ is some high-energy scale. As such, we expect the Majorana mass to be smaller than V . The diagonalization of the squared mass matrix will yield two mass eigenstates, ν_A and ν_S . We will assume that the active neutrino ν_A is mostly ν_L , with only a small mixing of ν_R .

The interactions in the gauge sector can be explored by defining the covariant derivative as,

$$D_\mu \mathbb{I} = \partial_\mu \mathbb{I} + i\frac{g}{2}\tau_a W_{\mu a} + ig'Y B_\mu + i\frac{g_{T_{3R}}}{2}Q_{T_{3R}}A'_\mu. \quad (3)$$

where g , g' and $g_{T_{3R}}$ represent the coupling constants of the $SU(2)_L$, $U(1)_Y$ and $U(1)_{T_{3R}}$ groups, respectively. The respective gauge bosons are denoted by W_μ , B_μ and A'_μ . The mass of the dark photon, A' , can be obtained from $|D_\mu \phi|^2$ as $m_{A'}^2 = 2g_{T_{3R}}^2 V^2$. The interactions involving the gauge boson A' are then given by,

$$\mathcal{L}_{\text{gauge}} = \frac{m_{A'}}{4\sqrt{2}V}A'_\mu(\bar{\eta}_1\gamma^\mu\eta_2 - \bar{\eta}_2\gamma^\mu\eta_1) + \frac{m_{A'}^2}{V\sqrt{2}}\phi'A'_\mu A'^\mu + \frac{m_{A'}^2}{4V^2}\phi'\phi'A'_\mu A'^\mu - \frac{m_{A'}}{2\sqrt{2}V}j_{A'}^\mu A'_\mu. \quad (4)$$

where the interaction current for the SM fermions is defined as, $j_{A'}^\mu = \sum_f Q_{T_{3R}}^f \bar{f}\gamma^\mu (\frac{1+\gamma_5}{2}) f$. Note that the η fields have only off-diagonal vector interaction with A' .

All the SM fermion masses and the DM masses are proportional to the symmetry breaking scale V , and their masses are $\lesssim V$. If we assume that there is no other suppression due to any other flavor physics, $V = \mathcal{O}(1)$ GeV would naturally give rise to sub-GeV masses for the fermions with $\mathcal{O}(1)$ Yukawa couplings. But this would be ruled out by the current constraints. Therefore we choose the symmetry breaking scale to be $V = 10$ GeV, leading to couplings which are moderately smaller than $\mathcal{O}(1)$. The dark photon and the dark Higgs masses will also be $\leq \mathcal{O}(1)$ GeV.

If $m_{\nu_S} > 2m_\mu$, then the tree-level decay process $\nu_S \rightarrow \mu^+\mu^-\nu_A$ will occur rapidly. For $m_{\nu_S} < 2m_\mu$, the sterile neutrino ν_S can decay via the process $\nu_S \rightarrow \nu_A\gamma\gamma$, with a rate

$$\Gamma_{\nu_S} \propto \alpha_{em}^2 \frac{m_{\nu_S}^7 m_{\nu_D}^2}{m_{\phi'}^4 V^4}. \quad (5)$$

For $V = 10$ GeV, $m_{\phi'} \sim 100$ MeV, $m_{\nu_S} = 10$ MeV, $m_{\nu_D} = 10^{-3}$ MeV we find $\tau_{\nu_S} \sim \mathcal{O}(10^{13})$ s. So we may essentially assume that the light sterile neutrino is stable for the purpose of laboratory experiments, though it need not be cosmologically stable. For points in parameter space at which the sterile neutrino is very light, it will also be a dark matter component. Note, the $\nu_S \rightarrow \nu_A\gamma$ decay process is also possible through a transition dipole interaction, but this process arises at two loop level and is therefore highly suppressed. This decay cannot proceed through a vector interaction, as a result of gauge invariance.

II.I Corrections to $g - 2$

Note that the muon anomalous magnetic moment will receive corrections arising from diagrams in which either ϕ' or A' run in the loop. The correction to $a_\mu = (g_\mu - 2)/2$ due to one-loop diagrams involving A' and ϕ' is given by [9]

$$\Delta a_\mu = \frac{m_\mu^4}{16\pi^2 V^2} \int_0^1 dx \frac{(1-x)^2(1+x)}{(1-x)^2 m_\mu^2 + x m_{\phi'}^2} + \frac{m_\mu^2}{32\pi^2 V^2} \int_0^1 dx \frac{2x(1-x)(x-2)m_{A'}^2 - 2x^3 m_\mu^2}{x^2 m_\mu^2 + (1-x)m_{A'}^2}. \quad (6)$$

But it is important to note that $g_\mu - 2$ can also receive corrections from high-scale physics which is disconnected from the dark sector. As such, $g_\mu - 2$ really constrains the amount of fine-tuning which is needed in order to match the data. As shown in [4], the allowed parameter space for this model would require a fine-tuning against high-scale physics at the 1% level if $V = 10$ GeV. This would be reduced to 10% if we instead adopted $V = 30$ GeV.

II.II A' Interactions and Decays

The dark photon has a tree-level coupling to some right-handed SM fermions (u_R , d_R , μ_R and ν_R), with coupling strength given by,

$$g_{T_{3R}} = \frac{m_{A'}}{\sqrt{2}V}. \quad (7)$$

The relation between $g_{T_{3R}}$ and $m_{A'}$ is shown in Fig. 1 for various choices of V .

The A' has a vector coupling to all other charged SM fermions, with coupling given by ϵe , where ϵ is a kinetic mixing parameter. The kinetic mixing parameter receives a one-loop contribution from the right-handed fermions charged under $U(1)_{T_{3R}}$ ($\sim g_{T_{3R}}\sqrt{\alpha_{em}/4\pi^3}$), as shown in Fig. 2.

But ϵ can also receive a tree-level contribution in the low-energy effective field theory. One source of these contributions could be the integrating out of heavy degrees of freedom which are also charged under $U(1)_{T_{3R}}$. We will thus consider the kinetic mixing parameter ϵ to be a free parameter.

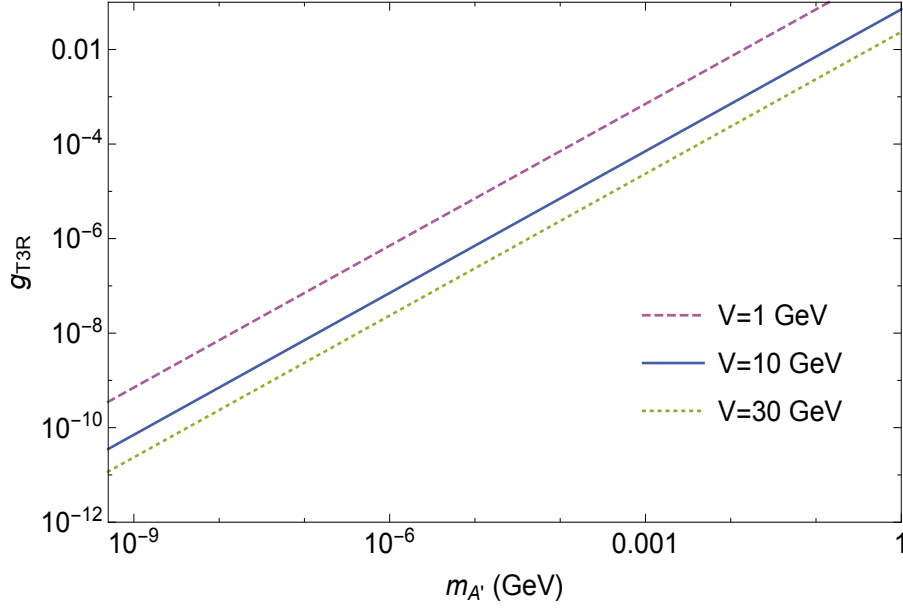


Figure 1: The relation between the coupling constant g_{T3R} and the gauge boson mass $m_{A'}$ for three different values of $V = 1, 10, 30$ GeV. For phenomenological study we set the value $V = 10$ GeV in rest of the paper.

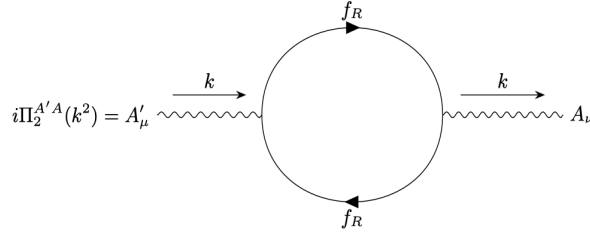


Figure 2: The one loop diagrams which give the mixing induced coupling between the SM fields to A' . Here, $f_R = \mu_R, u_R, d_R$.

A' also has an off-diagonal coupling to the vector current

$$j_\eta^\mu = \frac{1}{2}(\bar{\eta}_1 \gamma^\mu \eta_2 - \bar{\eta}_2 \gamma^\mu \eta_1). \quad (8)$$

Note, this coupling can only be off-diagonal, because it descends from a vector coupling to $\eta_{L,R}$. This Dirac fermion splits into two Majorana fermions as a result of symmetry-breaking, but the diagonal vector current for a Majorana fermion vanishes identically.

Since we take the A' to be lighter than $2m_\mu$ in order to avoid bounds from BaBar [10, 11], the only potentially allowed two-body final states are $\eta_{1,2}\eta_{2,1}$, $\nu\nu$, and e^+e^- , of which only the last one is visible. Note, the decay $A' \rightarrow \gamma\gamma$ is forbidden by the Landau-Yang theorem [12, 13]. The relevant A' decay rates are

$$\begin{aligned} \Gamma_{\eta_1\eta_2}^{A'} &= \frac{m_{A'}^3}{96\pi V^2} \left(1 - \frac{4m_\eta^2}{m_{A'}^2}\right)^{1/2} \left(1 + \frac{2m_\eta^2}{m_{A'}^2}\right), \\ \Gamma_{\nu_S\nu_S}^{A'} &= \frac{m_{A'}^3}{12\pi V^2} \left(1 - \frac{4m_{\nu_S}^2}{m_{A'}^2}\right)^{3/2}, \\ \Gamma_{e^+e^-}^{A'} &= \frac{\epsilon^2 \alpha_{em} m_{A'}}{3} \left(1 - \frac{4m_e^2}{m_{A'}^2}\right)^{1/2} \left(1 + \frac{2m_e^2}{m_{A'}^2}\right). \end{aligned} \quad (9)$$

where we have assumed that $m_{\eta_2} - m_{\eta_1}$ is negligible. Note, A' has no visible two-body decays if $m_{A'} < 2m_e$. If either the $\eta_1\eta_2$ or $\nu_S\nu_S$ final states are kinematically allowed, then those tree-level decays will dominate the branching fraction. Moreover, they will be prompt unless $m_{A'}$ is very small.

If neither of those states are kinematically allowed, then the dominant decays will be to either $\nu_S\nu_A$, $\nu_A\nu_A$, or e^+e^- . The first two of these are suppressed by powers of the mixing angle, while the last is suppressed by the kinetic mixing parameter.

II.III ϕ' Interactions and Decays

ϕ' couples to the SM fermions charged under $U(1)_{T3R}$, as well as to η_1 and η_2 , with a coupling given by $m_f/\sqrt{2}V$. ϕ' couples to $\nu_L\nu_R$ with a coupling given by $m_{\nu_D}/\sqrt{2}V$, where m_{ν_D} is the neutrino Dirac mass.

ϕ' can decay to $\mu^+\mu^-$, $\eta\eta$, $\nu\nu$, $A'A'$ and $\gamma\gamma$. The first and the last of these are visible, and the last one occurs only at one-loop. Decays to ν_S or A' can also produce visible energy, if those states in turn decay to SM particles. Tree-level decays to hadronic states are also possible if $m_{\phi'} > 2m_\pi$, but the branching fraction to these states is negligible compared to $\mu^+\mu^-$, because the coupling to first-generation quarks is so small.

The decay rates are

$$\begin{aligned}
\Gamma_{A'A'}^{\phi'} &= \frac{m_{\phi'}^3}{128\pi V^2} \left(1 - \frac{4m_{A'}^2}{m_{\phi'}^2}\right)^{1/2} \left(1 + 12\frac{m_{A'}^4}{m_{\phi'}^4} - 4\frac{m_{A'}^2}{m_{\phi'}^2}\right), \\
\Gamma_{\mu^+\mu^-}^{\phi'} &= \frac{m_\mu^2 m_{\phi'}}{16\pi V^2} \left(1 - \frac{4m_\mu^2}{m_{\phi'}^2}\right)^{3/2}, \\
\Gamma_{\eta_i\eta_i}^{\phi'} &= \frac{m_{\eta_i}^2 m_{\phi'}}{32\pi V^2} \left(1 - \frac{4m_{\eta_i}^2}{m_{\phi'}^2}\right)^{3/2}, \\
\Gamma_{\nu_S\nu_A}^{\phi'} &= \frac{m_{\nu_D}^2 m_{\phi'}}{16\pi V^2} \left(1 - \frac{m_{\nu_S}^2}{m_{\phi'}^2}\right)^2, \\
\Gamma_{\gamma\gamma}^{\phi'} &= \frac{\alpha_{em}^2 m_\mu^4}{8\pi^3 m_{\phi'} V^2} \left[1 + \left(1 - \frac{4m_\mu^2}{m_{\phi'}^2}\right) \left(\sin^{-1} \frac{m_{\phi'}}{2m_\mu}\right)^2\right]^2,
\end{aligned} \tag{10}$$

where we have computed $\Gamma_{\gamma\gamma}^{\phi'}$ only under the assumption $m_{\phi'} < 2m_\mu$ (otherwise, this decay is negligible compared to the $\mu^+\mu^-$ channel). Note that the decay $\phi' \rightarrow \gamma\gamma$ is always kinematically allowed, and (for $m_{\phi'} = 100$ MeV) will occur at a rate $\sim \mathcal{O}(10^{12})\text{s}^{-1}$.

Note also that, if $m_{\phi'} > 2m_{A'}$, then ϕ' can decay promptly to A' . But if this decay channel is dominant, then ϕ' production in a beam experiment is essentially no different from A' production, and can be searched for using strategies for detecting A' production.

II.IV Longitudinal Polarization of A'

When the gauge group is $U(1)_{T3R}$, which couples to chiral fermions, there is one aspect of the A' coupling to matter which is qualitatively different from other cases (such as $U(1)_{B-L}$, $U(1)_{L_i-L_j}$, $U(1)_X$ [18, 19, 20, 21, 22]) and which can have a major impact on experimental sensitivity. In particular, there can be an enhancement in the production of the A' longitudinal polarization.

The longitudinal polarization vector is $\propto E_{A'}/m_{A'} \propto E_{A'}/g_{T3R}V$. This yields an enhancement to the matrix element for processes wherein the longitudinal mode is produced at high-boost. For such processes, by the Goldstone Equivalence theorem, the matrix element is similar to that for production of the Goldstone boson of $U(1)_{T3R}$ symmetry-breaking, with a coupling to fermions which goes as $m_f/\sqrt{2}V$. For small $m_{A'}$, the coupling of a SM fermion to the longitudinal polarization is enhanced with respect to the transverse polarizations by a factor $m_f/m_{A'}$. But this enhancement cannot be arbitrarily large, as it is limited by perturbative unitarity. Since $m_f < V = 10$ GeV, our scenario is perturbative.

Note that this enhancement only comes into play because the A' couples to chiral SM fermions. The vector part of the interaction vanishes identically for a longitudinally-polarized A' , due to the Ward identity, and the enhanced matrix element arises entirely from the axial part. As a result, the enhancement in A' production occurs only for chiral models such as $U(1)_{T3R}$, not vector-like models such as $B-L$, L_i-L_j , etc.

As a result, the A' production cross section is only enhanced if the A' is produced at tree-level. If A' is produced through kinetic mixing, then the contribution from longitudinal polarization will again vanish identically due to the Ward Identity. Although there is an enhancement of processes where A' is produced through a coupling to u -/ d -quarks, one can see from the Goldstone Equivalence theorem that, even for small $m_{A'}$, this process can be approximated by the production of a massless pseudoscalar with coupling $m_q/\sqrt{2}V \lesssim 10^{-3} - 10^{-4}$. The most dramatic effect will be on production of the A' through a coupling to muons as the coupling to u -/ d -quarks is suppressed by close to two orders of magnitude, compared to the coupling to muons. This will be relevant for cosmological production (via $\mu^+\mu^- \rightarrow \gamma A'$), production in supernovae (which have non-negligible muon content), and from future experiments involving the invisible decays of light A' coupling directly to muons, such as NA64 μ and LDMX-M³.

Invisible final states: Astrophysical/cosmological bounds

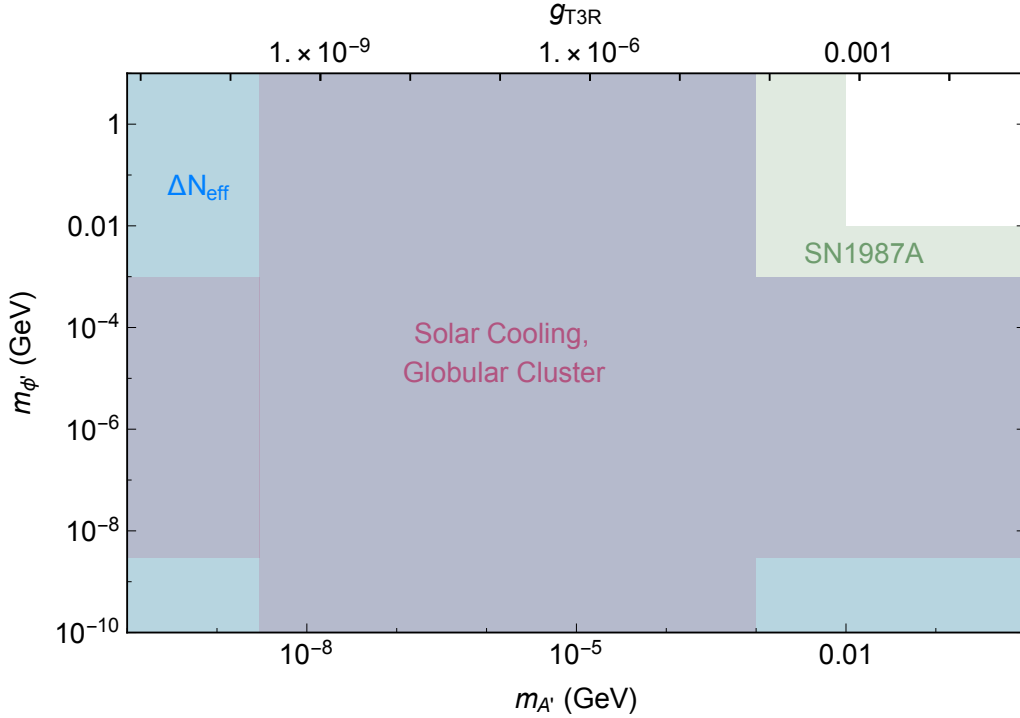


Figure 3: Constraints arising from cosmological and astrophysical observables, assuming that the A' and ϕ' decay to invisible states. These include constraints on ΔN_{eff} (green region) [7], on excess cooling of stars [14, 15] and globular clusters (gray region) [14], and excess cooling of supernovae (light green region) [16, 17]. The astrophysical bounds, however, are model dependent as mentioned in the text.

III Cosmological and Astrophysical Constraints

There are a variety of constraints on new physics models which arise from cosmological and astrophysical observables.

For example, if the Universe reheats to a temperature $\gtrsim 100$ MeV, then models with $m_{A'} < 1$ MeV and $V \sim \mathcal{O}(10)$ GeV are ruled out, because they would lead to a number of effective neutrinos (N_{eff}) [7] which is inconsistent with CMB measurements [23]. But this bound is circumvented if the Universe reheats to a lower temperature.

Note that if the right-handed electron were charged under $U(1)_{T3R}$, then models with $m_{A'} < 1$ MeV would similarly be ruled out by constraints on N_{eff} . But this constraint cannot be evaded by reheating to a lower temperature; to avoid this constraint, one would have to reheat to a temperature below 1 MeV, but this is ruled out by BBN.

Similarly, a variety of new constraints have recently been shown to arise from bounds on supernovae cooling [16, 17]. Essentially, the temperature of supernovae is large enough that a non-negligible population of muons is produced, and if they couple to new scalars or gauge bosons which decay invisibly, then there may be an anomalous rate of supernova cooling which would be ruled out by observations of SN1987A. But for $m_{A',\phi'} \gtrsim 10$ MeV, the mediators will decay promptly, and the decay products will be unable to free-stream out of the supernova.

White dwarf (WD) cooling constraints are negligible if $m_\eta, m_{\nu_s} \geq 0.1$ MeV, in which case they will be in equilibrium with the plasmons inside the WD and can not escape. The other possible final states are e^+e^- which is not allowed kinematically and $\nu_A\nu_A$, which is mixing angle suppressed [24]. We show constraint from solar cooling [14, 15] and cooling of stars in Globular clusters [14]

If Fig. 3, we plot these cosmological and astrophysical bounds on the $(m_{A'}, m_{\phi'})$ parameter space, in the case where A' and ϕ' decay invisibly. Note that there are no constraints plotted in the case where $m_{A'}, m_{\phi'} > 200$ MeV, because in this case, decays to $\mu^+\mu^-$ necessarily occur at tree-level. However, this region of parameter space is already ruled out by BaBar, as we will see later.

All the astrophysical constraints, however, can be evaded by assuming dark photon to be chameleon-type field with its mass depending on the environmental matter density [25, 26, 27, 14].

Visible final states: Current laboratory bounds

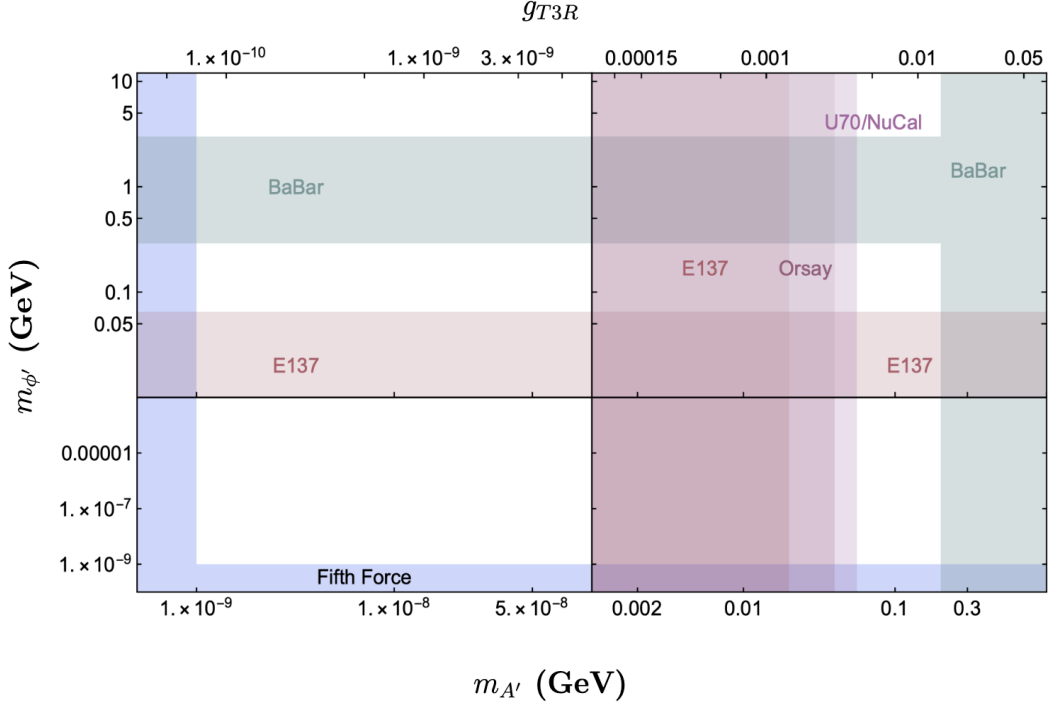


Figure 4: Regions of parameter space excluded by current laboratory experiments, assuming that A' and ϕ' decay dominantly to SM particles. Included are bounds from BaBar [10, 11, 28], E137 [29, 30, 31], Orsay [32, 28], U70/NuCal [33, 32, 28] and from fifth force experiments [34, 14].

IV Visible Decays at Displaced Detectors

One experimental strategy consists of producing light mediators at a proton collider, fixed-target, or beam dump experiment and searching for visible decays of this mediator at a distant detector. Upcoming experiments of this type include FASER [35, 36, 37, 38, 39], SHiP [40, 41], LDMX [42, 43, 44, 45, 46], and proposed modifications of SeaQuest [47, 48].

These experiments can only probe a model if the mediator is long-lived, and if it decays visibly. If the dominant decay of the A' is to e^+e^- through kinetic mixing, then the decay length may be long enough for the decay to occur within the detector. For the case of ϕ' , one must determine the rate of ϕ' production at the beam, which is beyond the scope of this work.

For most of these experiments, the production of A' will occur through p -bremsstrahlung and meson decay, where the A' couples at tree-level to u - and d -quarks. Since the A' can be produced with a significant boost, one might wonder if the enhancement to the production of the longitudinal polarization will be relevant. But the enhancement in the coupling to the Goldstone mode, relative to the transverse polarizations, scales as $m_f/m_{A'}$, and is only large when $m_{A'}$ is small. But visible decays are only possible for $m_{A'} > 1$ MeV. In any case, we will see that the limit of the sensitivity range for upcoming experiments will be $m_{A'} = \mathcal{O}(100)$ MeV, and for such high masses, the enhancement to the production rate of the longitudinal polarization is minimal. Indeed we will eventually see that the production enhancement for the longitudinal mode is most dramatic for invisible decays of light A' .

But although A' production is a tree-level process, A' decay occurs at one-loop through kinetic mixing. As a result, the sensitivity to our model can be estimated by considering the estimated sensitivity of these experiments to models where A' only couples to the SM via kinetic mixing, but with the number of events enhanced by the factor $(\pi/\alpha_{em}f)^2$, to account for the fact that A' production is a tree-level process. Here, f is the factor by which the kinetic mixing parameter exceeds that obtained only from one-loop diagrams with SM fermions in the loop.

The sensitivity of displaced detector experiments is dominated by A' produced at the largest energies, since these particles have the largest decay length (ℓ_{decay}). We will denote this characteristic energy as E , with $\ell_{decay} \propto (E/m_{A'})^2 \epsilon^{-2}$, assuming that the decay proceeds through an intermediate photon. We may then write $\ell_{decay}(m_{A'}) = (\epsilon_0(m_{A'})/\epsilon)^2 L$, where L is the distance from the beam to the front edge of the detector, and $\epsilon_0(m_{A'}) \propto m_{A'}^{-1}$ is a factor which is independent of ϵ .

If ϵ^{kin} is the value of kinetic mixing parameter (assuming A' couples to the SM only through kinetic mixing), then the expected number of A' which decay within a detector of length ΔL is given by

$$N_{kin} = C (\epsilon^{kin})^2 \left[e^{-(\epsilon^{kin}/\epsilon_0)^2} - e^{-(\epsilon^{kin}/\epsilon_0)^2(1+\Delta L/L)} \right], \quad (11)$$

where C is a constant which depends on the details of the experiment, but is independent of ϵ and $m_{A'}$. For the dark photon of $U(1)_{T3R}$, since the A' is produced at tree-level, the expected number of A' decaying within the detector would instead be given by

$$N_{T3R} = C \left(\frac{\pi}{\alpha_{em} f} \right)^2 (\epsilon^{T3R})^2 \left[e^{-(\epsilon^{T3R}/\epsilon_0)^2} - e^{-(\epsilon^{T3R}/\epsilon_0)^2(1+\Delta L/L)} \right], \quad (12)$$

If we denote by \bar{N} the number of decaying A' which could be statistically detected above background, then the excluded region consists of points for which $N_{kin, T3R} > \bar{N}$.

The sensitivity of experiments of this type have a ceiling and floor; below the floor, the coupling is too weak for enough A' to be produced, while above the ceiling, the A' decays too rapidly to reach the detector. For a kinetic mixing parameter at the floor of sensitivity (ϵ_-), we may assume $\ell_{decay} \gg L > \Delta L$, which implies that $(\epsilon_-/\epsilon_0)^2(\Delta L/L) \ll 1$.

If $\epsilon_-^{kin}(m_{A'})$ is the floor of the sensitivity region of an experiment for the secluded model, then

$$\bar{N} = C (\epsilon_-^{kin})^2 \left(\frac{\epsilon_-^{kin}}{\epsilon_0} \right)^2 \frac{\Delta L}{L}. \quad (13)$$

The sensitivity floor of the $U(1)_{T3R}$ model is given by the solution to the equation

$$\left(\frac{\pi}{\alpha_{em} f} \right)^2 \left(\frac{\epsilon_-^{T3R}}{\epsilon_-^{kin}} \right)^4 = 1, \quad (14)$$

which is obtained by setting $N_{T3R} = \bar{N}$.

For values of kinetic mixing at the ceiling of sensitivity (ϵ_+), we may assume that $\ell_{decay} \ll \Delta L$, or equivalently $(\epsilon_+/\epsilon_0)^2(\Delta L/L) \gg 1$. If $\epsilon_+^{kin}(m_{A'})$ is the ceiling of the sensitivity region of an experiment for the secluded model (where all dark photon interactions proceed through kinetic mixing), then we find

$$\bar{N} = C (\epsilon_+^{kin})^2 e^{-(\epsilon_+^{kin}/\epsilon_0)^2}. \quad (15)$$

The ceiling of the $U(1)_{T3R}$ model is given by the solution to the equation

$$\left(\frac{\pi}{\alpha_{em} f} \right)^2 \left(\frac{\epsilon_+^{T3R}}{\epsilon_+^{kin}} \right)^2 \exp \left[[(\epsilon_+^{kin})^2 - (\epsilon_+^{T3R})^2] / \epsilon_0^2 \right] = 1, \quad (16)$$

which is again obtained by setting $N_{T3R} = \bar{N}$.

To solve this equation, we must solve for $\epsilon_0(m_{A'})$. To do this, we can use the fact that, for the secluded model, the expected number of A' decaying in the detector is \bar{N} when the kinetic mixing parameter is either ϵ_-^{kin} or ϵ_+^{kin} , yielding the relation

$$(\epsilon_+^{kin})^2 \exp[-(\epsilon_+^{kin})^2/\epsilon_0^2] = \frac{(\epsilon_-^{kin})^4}{\epsilon_0^2} \frac{\Delta L}{L}. \quad (17)$$

Given $\epsilon_{\pm}^{kin}(m_{A'})$ from an experimental sensitivity or constraint curve, one can use the above relation to solve for $\epsilon_0(m_{A'})$, and in turn determine $\epsilon_{\pm}^{T3R}(m_{A'})$. But if visible decays are kinematically allowed at all, then we must have $m_{A'} > 1$ MeV; taking $V = 10$ GeV, we find that we must have $g_{T3R} \gtrsim 10^{-4}$.

If we assume that kinetic mixing is generated at one-loop only by SM fermions (that is, $f = 1$) then we find that the following bounds (from U70/NuCal) and future sensitivities :

- U70/NuCal: Ruled out if $1 \text{ MeV} \lesssim m_{A'} \lesssim 56 \text{ MeV}$
- FASER: Probed if $1 \text{ MeV} \lesssim m_{A'} \lesssim 86 \text{ MeV}$
- FASER-2 and SHiP (their sensitivities are similar): Probed if $1 \text{ MeV} \lesssim m_{A'} \lesssim 96 \text{ MeV}$
- SeaQuest: Probed if $1 \text{ MeV} \lesssim m_{A'} \lesssim 109 \text{ MeV}$

Visible final states: Future laboratory bounds

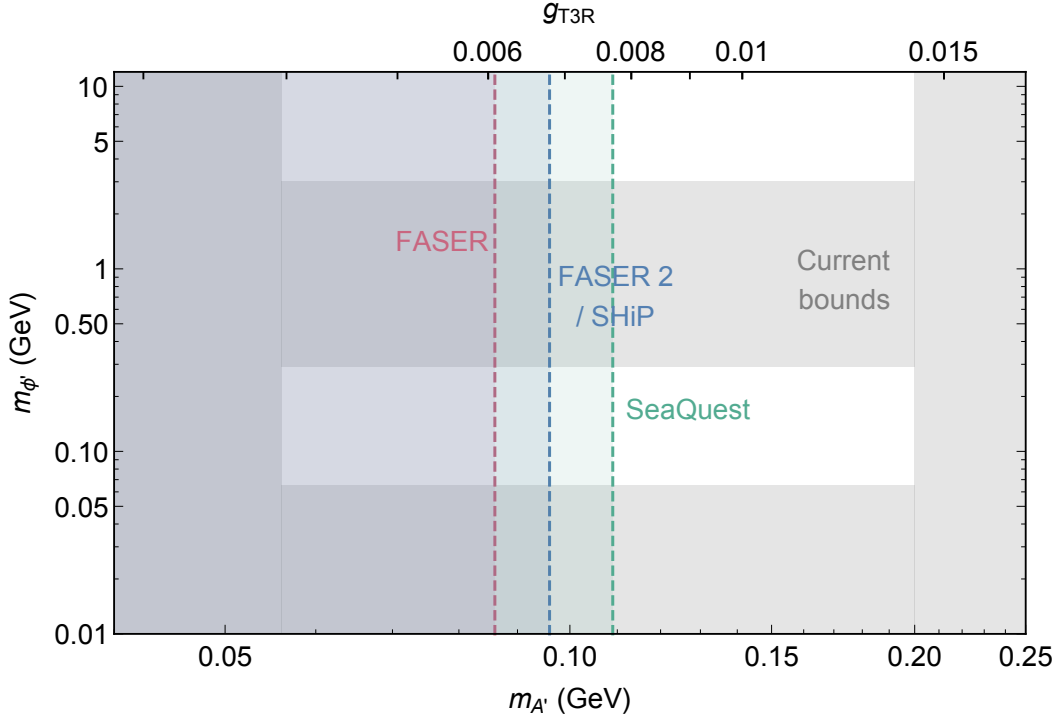


Figure 5: The sensitivity of upcoming laboratory experiments to A' , ϕ' decay at displaced detectors. Shown are the sensitivities of FASER [39] (purple region), FASER 2/SHiP [39] (dark green region), and SeaQuest [47] (light green region). Also shown are constraints from current laboratory experiments (light gray region), reproduced from Fig. 4.

Note that, since the gauge coupling scales as $\propto m_{A'}/V$, increasing V actually increases the mass reach, by increasing the decay length.

There are also a variety of current electron beam dump experiments which can constrain this scenario [4]. For these experiments, one-loop processes can result in the production of either A' (kinetic-mixing) or ϕ' (Primakoff production), with subsequent one-loop decays to SM particles at a displaced detector.

There are some other constraints on this scenario from current laboratory experiments, which were discussed in [4]. In particular, BaBar [10, 11] provides tight constraints on the regions of parameter space where $e^+e^- \rightarrow \mu^+\mu^- (A', \phi' \rightarrow \mu^+\mu^-)$ is kinematically accessible. Regions of parameter space in which either ϕ' or A' are extremely light are also tightly constrained by fifth force experiments [34]. Note that, although $g_{T3R} \propto m_{A'}$, regions of parameter space with very small $m_{A'}$ are still tightly constrained by fifth force experiments; although the transverse modes of the A' decouple as $m_{A'} \rightarrow 0$, the Goldstone mode still contributes to the fifth force.

In Fig. 4, we plot constraints on this scenario from current laboratory experiments in the $(m_{A'}, m_{\phi'})$ -plane, where we assume that A' , ϕ' predominantly decay to SM particles. In particular, we plot constraints from BaBar [10, 11, 28], E137 [29, 30, 31], Orsay [32, 28], U70/NuCal [33, 32, 28] and from fifth force experiments [34, 14]. If they decay instead dominantly to invisible states, then these bounds are weakened considerably. In Fig. 5, we plot projected bounds arising from visible decay at displaced detectors such as FASER, FASER-2 [35, 36, 37, 38, 39], SHiP [40, 41] and SeaQuest [47, 48] in the $(m_{A'}, m_{\phi'})$ -plane.

V Visible and Invisible Decays at Nearby detectors

The Crystal Barrel (CB) [54, 55] detector can give constraints on $m_{A'}$ when A' predominantly decays to invisible final states. CB set an upper limit of the branching ratios (Br) for the process $P \rightarrow \gamma X$, where $P = \pi^0, \eta, \eta'$ and X is a boson which is either long-lived, or decays invisibly. We consider $X = A'$, the dark photon. The parameter space probed for the η and η' decay will be ruled out by other experiments. We mainly look at π^0 decay. The bound from CB is [54, 55],

$$\text{Br}(\pi^0 \rightarrow \gamma A') \leq 2.8 \times 10^{-4}, \quad m_{A'} \leq 65 \text{ MeV}, \quad (18)$$

and,

$$\text{Br}(\pi^0 \rightarrow \gamma A') \leq 6.0 \times 10^{-5}, \quad 65 \text{ MeV} \leq m_{A'} \leq 125 \text{ MeV}, \quad (19)$$

Invisible final states: Current laboratory bounds

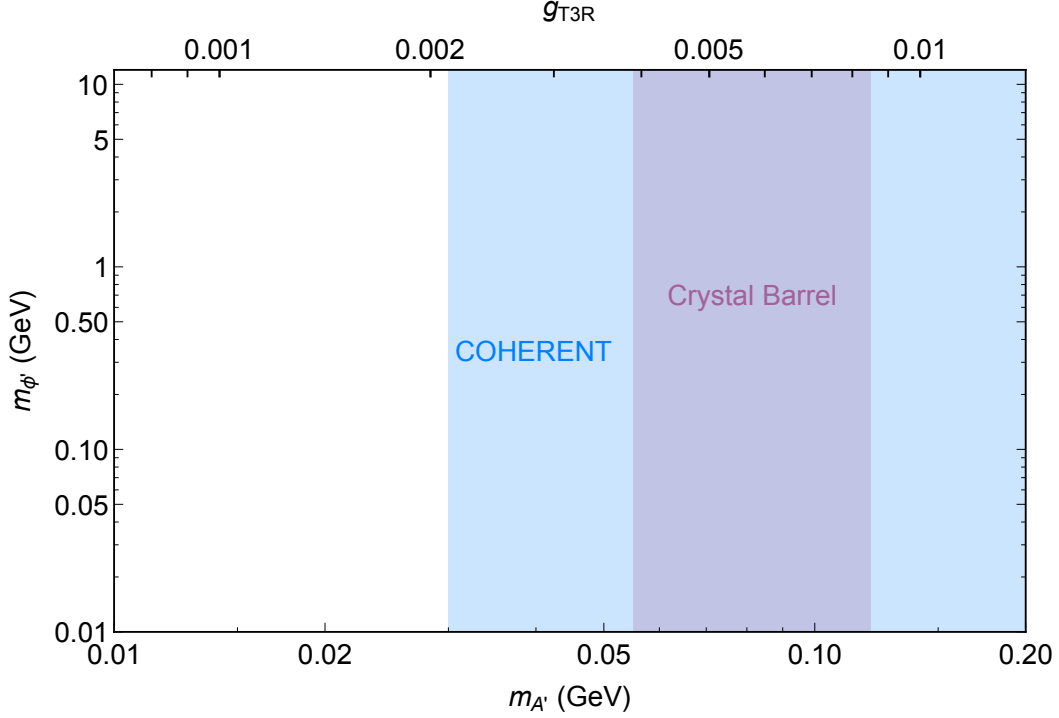


Figure 6: Regions of parameter space excluded by current laboratory experiments, assuming that A' and ϕ' decay dominantly to invisible final states. Included are bounds from the COHERENT [49, 50, 51, 52, 53] (light blue) and Crystal Barrel [54, 55] (light purple) experiments.

The branching fraction for our model is given by

$$\text{Br}(\pi^0 \rightarrow \gamma A') = \frac{m_{A'}^2}{4\pi\alpha V^2} \left(1 - \frac{m_{A'}^2}{m_{\pi^0}^2}\right)^3 \quad (20)$$

Therefore the region of parameter space, $55 \text{ MeV} < m_{A'} < 120 \text{ MeV}$ will be ruled out by CB.

Proposed detectors such as NA64 μ [56, 57] and LDMX-M³ [58, 46] (a proposed muon beam version of LDMX [43]) can probe this scenario in the case where either A' or ϕ' has a significant decay rate to invisible states. NA64 μ proposes to collide a muon beam with a target, and search for interactions with missing energy. In the case of a scalar mediator which does not decay to visible energy within the detector, it is estimated that NA64 μ could probe muon-scalar couplings $\sim \mathcal{O}(10^{-5})$, largely independent of the scalar mass [56]. The coupling of ϕ' to muons is $\mathcal{O}(10^{-2})$, implying that this scenario can be probed by NA64 μ for any $m_{\phi'}$, provided the branching fraction to invisible states satisfies $\text{Br}(\text{invisible}) > 10^{-6}$. Note that, in the scenario in which ϕ' couples to muons at tree-level, LDMX-M³ Phase 1 will probe any $m_{\phi'}$, provided $\text{Br}(\text{invisible}) > 10^{-4}$, while Phase 2 will have a greater sensitivity than NA64 μ [46].

Since the decay $\phi' \rightarrow \gamma\gamma$ is one-loop suppressed, whereas the decays $\phi' \rightarrow \nu_S \nu_A, \eta\eta$ occur at tree-level, these invisible decays will dominate if kinematically allowed. In fact, even if the decay $\phi' \rightarrow \mu^+ \mu^-$ is kinematically allowed, the invisible decays will still have a branching fraction of at least $\mathcal{O}(10^{-4})$, provided $m_{\eta, \nu_S} > 1 \text{ MeV}$. All these scenarios can thus be probed by NA64 μ and LDMX-M³.

Note that the sensitivity of NA64 μ to A' is roughly similar. Even for arbitrarily light A' (with arbitrarily weak coupling), the longitudinal mode couples to muons approximately the same as a pseudoscalar with coupling $\sim \mathcal{O}(10^{-2})$. We thus find that NA64 μ and LDMX-M³ will be able to probe the entire parameter space, provided $m_{A', \phi'} > 2m_\eta$ or $2\nu_S$.

Even if the $\eta\eta$ and $\nu_S \nu_S$ final states are not kinematically allowed, and the dominant decay of A' is to $e^+ e^-$, NA64 μ and LDMX-M³ will still be sensitive if the decay length of the A' is long enough that a significant number of A' leave the detector without decaying.

The sensitivity of NA64 μ to a minimally flavor-violating (MFV) scalar which couples to both muons and electrons was considered in [56], and this case is essentially the same as for the A' . But in that study it was assumed that the coupling of the mediator to electrons was suppressed relative to the coupling to muons by the factor (m_e/m_μ) , whereas we instead assume that is suppressed by the kinetic mixing factor $(\alpha_{em}/\pi)f$.

As with displaced detectors, the NA64 μ sensitivity region has a floor (below which not enough A' are

Invisible final states: Future laboratory bounds

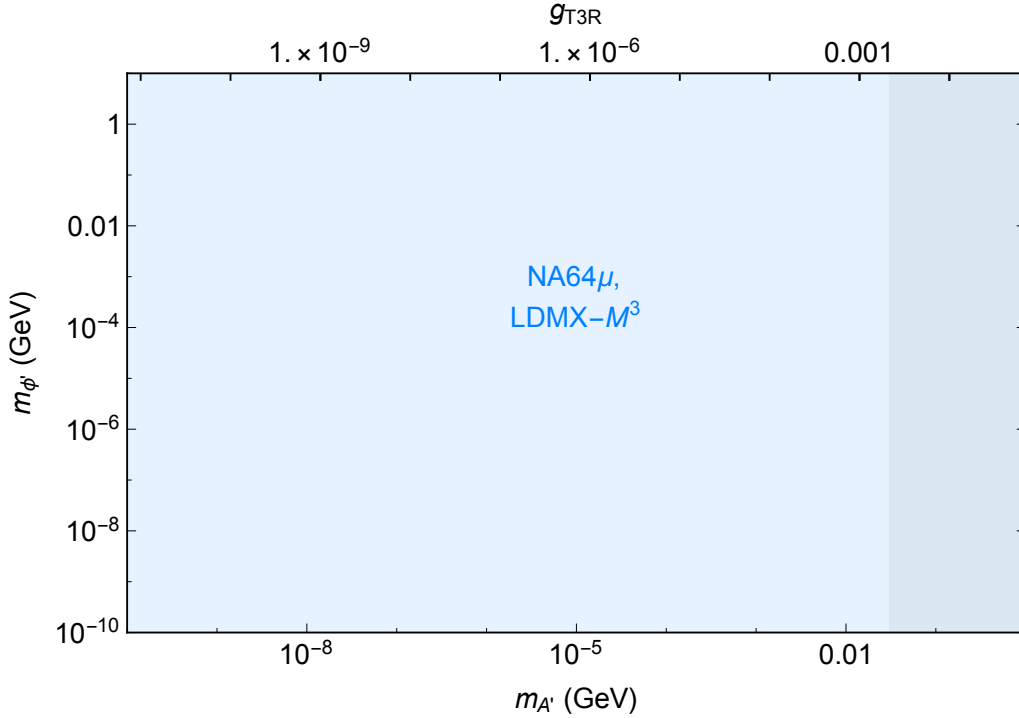


Figure 7: The sensitivity of upcoming laboratory experiments to the parameter space assuming that A' , ϕ' decay dominantly to invisible final states. Shown are the sensitivities of NA64 μ [56, 57], and LDMX- M^3 [58, 46] (light blue region). Also shown are constraints from current laboratory experiments (light gray region), reproduced from Fig. 6.

produced) and a ceiling (above which the A' decays to visible states within the detector). But because the coupling of the longitudinal polarization to muons is never smaller than $\mathcal{O}(10^{-2})$, our model is never below the floor for any choice of $m_{A'}$.

The ceiling of the NA64 μ sensitivity to the MFV scalar model can be translated into a sensitivity to the $U(1)_{T3R}$ model by rescaling the coupling by the factor $(m_e/m_\mu)(\pi/\alpha_{em}f) \sim 2.08f^{-1}$; this rescaling keeps the coupling to electrons (and thus the decay length) fixed, while increasing the A' production rate by an $\mathcal{O}(1)$ factor. Since decreasing the decay length causes an exponential suppression to the number of events, this simple rescaling is a good approximation. Applying this rescaling to the limits found in [56], we find that NA64 μ is sensitive to $U(1)_{T3R}$ models for which $m_{A'} < 77$ MeV. But if e^+e^- is the dominant final state, then the range $1 \text{ MeV} < m_{A'} < 56$ MeV is already ruled out by U70/NuCal. If $m_{A'} < 1$ MeV, then no two-body visible decays are allowed, and both NA64 μ and LDMX- M^3 will probe this scenario.

Finally, we note that LDMX- M^3 may have sensitivity even if dark matter decays to visible states within the target. Whereas NA64 μ relies entirely on calorimetry, LDMX relies on tracking, and the location of energy deposition within the calorimeter. Even if prompt decays, such as $\phi' \rightarrow \gamma\gamma$ occur within the target, LDMX may be able to use information from the tracker to distinguish this event from Standard Model background.

V.I Belle-II: $e^+e^- \rightarrow \gamma + \text{invisible}$

Since the dark photon can kinetically mix with the photon, Belle-II [59, 60, 28] can study the process $e^+e^- \rightarrow \gamma A'$. Its sensitivity is best if the A' decays invisibly [60, 28], since in that case the Standard Model rate is relatively small. For $m_{A'} \lesssim 200$ MeV, Belle-II will be able to probe models with $g_{T3R} \gtrsim 10^{-3}$, corresponding to $m_{A'} \gtrsim 30$ MeV.

VI Dark Matter and Sterile Neutrino Scattering at Displaced Detectors

There are a variety of stopped pion based experiments e.g., COHERENT [49, 50, 51, 52, 53], CCM [61, 62], JSNS² [63, 64, 65, 66, 67], etc. which are designed to produce neutrinos from a proton beam hitting a target, and

search for the neutral current scattering of these neutrinos at a distant detector. Among these experiments, the ongoing COHERENT and CCM experiments are CE ν NS [68, 69] experiments. The COHERENT experiment has observed 6.7σ (at CsI detector [49]) and 3.8σ (at LAr [53]) evidences of CE ν NS type events. However these experiments also produce a tremendous number of photons from proton, electron bremsstrahlung and meson decays [70]. These photons can then produce A' . If the decays $A' \rightarrow \eta\eta$, $\nu_S\nu_S$ are kinematically allowed, then they will occur promptly and dominate the A' branching fraction. The scattering of the dark matter or sterile neutrinos against nuclei can then be probed. Unlike NA64 μ and LDMX- M^3 , these neutrino experiments probe the appearance of dark matter/sterile neutrinos at the detector, which makes these neutrino experiments complimentary to the beam dump searches described before. The neutrinos from pion and muon decays produce backgrounds for such searches. However, utilizing the pulsed nature of the beam and the timing and the energy spectra of the recoiling nucleus, it has been shown recently that one can extract the dark matter signal from the neutrino background [5]. The current result from the COHERENT experiment actually yields a tighter constraint on the dark matter parameter space compared to MiniBooNE [71, 72, 73, 74], LSND [71, 75, 76], NA64 [56, 57] etc. In fact COHERENT CsI-data shows some excess ($\sim 2.4 - 3\sigma$) for A' mass $\lesssim 100$ MeV where the A' decays promptly to dark matter or sterile neutrino (in this model) [5]. In Ref. [5], photons from π^0 decays were studied, while in Ref. [70] bremsstrahlung photons were also included to investigate dark matter emerging from dark photon decay, with similar results.

The search for light dark matter/sterile neutrinos relies on kinematic features to distinguish the scattering of ν_S or η from that of active neutrinos produced from the beam via SM processes. SM processes will dominantly produce active neutrinos via stopped pion decay, yielding neutrinos with an energy of 30 MeV. But A' can decay in flight to $\nu_S\nu_S$ or $\eta\eta$, yielding much higher energy particles. This type of search was considered in detail in [70], and we can apply their general results to our scenario.

Note that if sterile neutrino scattering is mediated by the ϕ' , then it is exothermic, as the outgoing neutrino is active. But as the sterile neutrino will already be boosted, the change in the event rate is an $\mathcal{O}(1)$ factor.

To rescale the limits found in [70] to our scenario, we need only note that the dominant method for A' production in our scenario will be from direct coupling to u - or d -quarks. As such, the event rate is proportional to two powers of the coupling of A' to dark matter (from the squared scattering matrix element) and four powers of the coupling of the A' to first generation quarks (two from the squared scattering matrix element, and two from the squared A' production matrix element). The exception is JSNS², which looks for scattering against electrons; for this experiment, two powers of the coupling to first-generation quarks are replaced with the coupling to electrons.

With these rescalings, the event rate for the models considered in [70] can be directly related to the event rate in our scenario. To facilitate comparison with [70], we take $m_\eta/m_{A'}, m_{\nu_S}/m_{A'} = 1/3$, though deviations from this assumption will not affect sensitivity significantly.

If dark matter or sterile neutrino scattering is dominantly mediated by the A' , then from the analysis of [5], we find that the COHERENT excess can be reproduced for $g_{T3R} \sim 0.002$. For $V = 10$ GeV, this corresponds to $m_{A'} \sim 30$ MeV. This parameter space is not ruled out by any other available laboratory based experimental result. Since the event rate scales as g_{T3R}^6 , the dark photon mass range significantly above this benchmark mass is excluded by COHERENT data.

Note that the enhancement in coupling to the longitudinal mode is not relevant for spin-independent scattering, which is mediated by a purely vector interaction.

If dark matter scattering is instead mediated by the ϕ' , then the event rate is suppressed by the factor $g_{T3R}^{-4} m_\eta^2 m_{u,d,e}^2 / 2V^4$; as long as $m_\eta, m_{A'} \gtrsim 30$ MeV, these models can also be ruled out by COHERENT. Finally, if the A' predominantly decays to sterile neutrinos, which scatter off nuclei dominantly through ϕ' exchange, then COHERENT rules out models for which $m_{\nu_D} m_{A'} \gtrsim (30 \text{ MeV})^2$.

Note that there are regions of parameter space for which these bounds can be weakened. For example, changing $m_{\eta,\nu_S}/m_{A'}$ can effect the sensitivity by an $\mathcal{O}(1)$ factor, which could open up regions of parameter space at the edge of COHERENT's sensitivity. Similarly, if $m_{\eta,\nu_S}/m_{A'} \sim 1/2$, then for relatively heavy $m_{A'}$, scattering at the detector may be non-relativistic, leading to a suppression of the event rate. But note that CCM and JSNS² will have sensitivity which should improve on COHERENT. This dark photon invisible decay parameter space also can be probed at DUNE [77, 78, 79, 80, 81, 82].

Bounds from Crystal Barrel and COHERENT are shown in the $(m_{A'}, m_{\phi'})$ parameter space in Fig. 6, assuming that the A'/ϕ' dominantly decay to invisible states. We also show the future sensitivities of NA64 μ and LDMX- M^3 on the $(m_{A'}, m_{\phi'})$ parameter space in Fig. 7.

VII Non-Standard Interactions for Active Neutrinos

The A' and ϕ' can mediate non-standard interactions of active neutrinos with nuclei. A variety of constraints on such interactions have been found from oscillation effects, short and long baseline experiments, CE ν NS experiments etc. Constraints can be found by using a large family of NSI, but considering one or two of them

at a time [83], by reparameterizing the NSI down to a more phenomenological and pragmatically manageable subset based on model assumptions (for example, in Refs. [84, 85, 86]), or by considering all the NSIs from a large set at the same time [87].

If the momentum transfer in the scattering process is much smaller than the mediator mass, then the effect of the A' and ϕ' couplings can be approximated by dimension-6 effective operators:

$$\begin{aligned}\mathcal{O}_{A'} &= \frac{\sin^2 \theta}{2V^2} (\bar{\nu}_A \gamma^\mu P_L \nu_A) (\bar{q} \gamma_\mu P_R q), \\ \mathcal{O}_{\phi'} &= \frac{m_q^2 \sin \theta}{2V^2 m_{\phi'}^2} (\bar{\nu}_A P_L \nu_A) (\bar{q} P_R q),\end{aligned}\tag{21}$$

where θ is the neutrino mixing angle. Note that the coefficient of $\mathcal{O}_{A'}$ has two powers of the neutrino mixing angle, since A' couples to two right-handed neutrinos, whereas the coefficient of $\mathcal{O}_{\phi'}$ has only one power, as ϕ' couples to a right-handed and a left-handed neutrino.

The coefficients of these operators are bounded by current experiments to be of $\lesssim \mathcal{O}(10^{-5}) \text{ GeV}^{-2}$ [87], and future experiments could improve this bound by an order of magnitude. For $\mathcal{O}_{A'}$, current experiments require $\sin^2 \theta \lesssim \mathcal{O}(10^{-3})$ [87], while future experiments could probe values of $\sin^2 \theta$ which are an order of magnitude smaller. For $\mathcal{O}_{\phi'}$, current experiments require [87]

$$\sin \theta \lesssim [\mathcal{O}(10^{-3})] \left(\frac{m_{\phi'}}{5 \text{ MeV}} \right)^2,\tag{22}$$

with the sensitivity of upcoming experiments, e.g., DUNE [77, 78, 79, 80, 81, 82], Hyper-K [88, 89, 90, 91, 92, 93] etc. to $\sin \theta$ being up to an order of magnitude higher.

The sterile neutrino, ν_s , is mostly composed of the right-handed neutrino (ν_R), but with a small mixing with the active neutrino. Because of this mixing the sterile neutrino can be produced in laboratory experiments. ν_s can be searched for at the HUNTER [94] experiment by kinematic reconstruction of the electron capture decay of the radioactive atom ^{131}Cs . Similarly, the ν_s can potentially be searched for with the TRISTAN project of the KATRIN [95] experiment, where it can yield a kink-like distortion in the tritium beta decay spectrum if $m_{\nu_s} \sim \mathcal{O}(\text{keV})$.

VIII Conclusion

We have considered the scenario in which right-handed light SM fermions are charged under a new gauge group, $U(1)_{T3R}$. This scenario is of particular interest because it can tie the symmetry-breaking scale of $U(1)_{T3R}$ to that of the light SM fermions and of the dark sector. This scenario thus naturally leads to a new set of sub-GeV particles, including the dark matter, a sterile neutrino, a dark photon, and a dark Higgs. In this paper, we have focused on ways of probing this scenario with new data sets. We have focused on the case where the symmetry-breaking scale is taken to be 10 GeV, but the results do not change qualitatively if that scale is increased to $\sim 30 \text{ GeV}$, unless the A' decays primarily to visible states.

We have found that the optimal probe of this scenario depends on the details of the model. Our main results are shown in Figures 3-7, and a summary of these sensitivities is presented in Table 2. One distinct feature of this scenario which has an impact on search strategies is that the dark photon has a chiral coupling to some SM fermions, yielding an enhancement to tree-level production of the longitudinal polarization.

If the dark photon or dark Higgs have kinematically-allowed decays to dark matter or to sterile neutrinos, then those tree-level decay processes will be prompt. In that case, excellent sensitivity arises for the ongoing experiments such as COHERENT, CCM and JSNS², in which the A' is produced at a target hit by a proton beam, and the invisible decay products scatter off nuclei in a distant detector. Indeed, the current $2.4 - 3\sigma$ excess in the event rate at COHERENT could be explained by a 30 MeV dark photon which is produced from photons at the target and decays to either dark matter or sterile neutrinos, and which also mediates the scattering of these invisible particles with nuclei in the target. Constraints from COHERENT rule out larger masses ($m_{A'} \gtrsim 30 \text{ MeV}$). One can also find very fine-tuned regions of parameter space where COHERENT's sensitivity is weakened because the dark matter is slow-moving when it reaches the detector. But CCM and JSNS² will improve on the current COHERENT sensitivity. This dark photon parameter space also can be searched at DUNE.

Moreover, excellent detection prospects also lie with experiments such as NA64 μ and LDMX-M³, in which a muon beam is collided with a target, and one searches for invisible decays. These experiments can probe the entirety of currently available parameter space in which the ϕ' or A' decay invisibly, including the parameter space region $m_{A'} \lesssim 30 \text{ MeV}$. The searches for dark photon at the neutrino experiments are however complimentary to the searches at NA64 μ and LDMX-M³ since the former investigates the appearance of dark matter/sterile neutrinos at the detector compared to the disappearance searches at the latter facilities. Belle-II can also probe models with $m_{A'} \gtrsim 30 \text{ MeV}$.

If the dark photon or dark Higgs decay largely to visible states, then the best prospects lie with beam experiments which search for visible decays in a distant detector, such as FASER, SeaQuest, and SHiP. These models provide excellent detection prospects, provided the mediating particle has a decay length long enough to reach the detector. These experiments can probe dark photons in the $\mathcal{O}(1 - 100 \text{ MeV})$ range, though there is still open parameter space at relatively large dark photon mass which these upcoming experiments cannot probe.

Cosmological and astrophysical observables can also play an important role. These constraints are especially interesting because, even for arbitrarily small gauge coupling, the longitudinal polarization of the dark photon has a large coupling to muons. In particular, if the Universe reheats to a temperature greater than $\mathcal{O}(100 \text{ MeV})$, then the entire parameter space with $m_{\phi', A'} \lesssim 1 \text{ MeV}$ can be ruled out. Similarly, observations of SN1987A can rule out scenarios in either $m_{\phi', A'} \lesssim 10 \text{ MeV}$, and has a dominant decay to dark matter or sterile neutrinos, though these supernovae constraints are subject to large systematic uncertainties, and can be weakened by chameleon effects, or other features of a more complicated dark sector.

We see that there is a rich and interesting phenomenology associated with scenarios in which light right-handed SM fermions are charged under a new gauge group, $U(1)_{T_{3R}}$, with low-mass mediators. This scenario is tightly constrained, yet there are still unexplored regions of parameter space.

The region of parameter space which will not be tested with upcoming experiments is where the dark photon and dark Higgs have dominantly visible decays, but with a decay length which is too short to reach upcoming displaced detectors. It would be interesting to consider new strategies for closing this remaining window, including shorter decay regions.

Table 2: A summary of the various experiments/probes considered here, their methods for producing and detecting the mediating particles, and the resulting sensitivities.

Type of experiments	Name of the experiment	Production of A'/ϕ'	Final states	Results
Electron beam dump experiments	E137, Orsay	A' : electron bremsstrahlung through kinetic mixing at one-loop, ϕ' : Primakoff production at one-loop.	Both A', ϕ' decay predominantly to visible SM states e^+e^- . ϕ' decay is rapid.	E137 rules out : $1 \text{ MeV} \leq m_{A'} \leq 20 \text{ MeV}$, $1 \text{ MeV} \leq m_{\phi'} \leq 65 \text{ MeV}$. Orsay rules out : $1 \text{ MeV} \leq m_{A'} \leq 40 \text{ MeV}$. U70/NuCal rules out : $1 \text{ MeV} \leq m_{A'} \leq 93 \text{ MeV}$.
Proton beam dump experiments	U70/NuCal, FASER SHiP, SeaQuest (displaced detector)	p -bremsstrahlung or meson decay at tree level	$A' \rightarrow e^+e^-$ through kinetic mixing. $\phi' \rightarrow \gamma\gamma$ ϕ' decays rapidly hence cannot be probed.	FASER can probe : $1 \text{ MeV} \leq m_{A'} \leq 140 \text{ MeV}$. FASER 2/SHiP can probe : $1 \text{ MeV} \leq m_{A'} \leq 161 \text{ MeV}$. SeaQuest can probe : $1 \text{ MeV} \leq m_{A'} \leq 180 \text{ MeV}$.
e^+e^- collider experiments	BaBar, Belle-II	$e^+e^- \rightarrow \mu^+\mu^- + A'/\phi'$, $e^+e^- \rightarrow \gamma A'$	4μ final states, γ + invisible	BaBar rules out for (4μ final states) : $200 \text{ MeV} \leq m_{A'} \leq 1.3 \text{ GeV}$, $290 \text{ MeV} \leq m_{\phi'} \leq 3 \text{ GeV}$. Belle-II can probe (γ + invisible): $m_{A'} \geq 30 \text{ MeV}$.
$\bar{p}p$ collider experiments	Crystal Barrel	$\bar{p}p \rightarrow \pi^0\pi^0\pi^0$, $\pi^0 \rightarrow \gamma A'$	invisible states	The parameter space is ruled out for: $55 \text{ MeV} < m_{A'} < 120 \text{ MeV}$
Fifth force searches experiments	Precision tests of gravitational Casimir, and van der Waals forces	Relevant for extremely light A'/ϕ' . For $m_{A'} \rightarrow 0$ limit, the Longitudinal mode will contribute.	n/a	The parameter space is ruled out for: $m_{A'}/m_{\phi'} \leq 1 \text{ eV}$. SN1987A rules out : $m_{A'}, m_{\phi'} \leq 200 \text{ MeV}$.
Astrophysical probes	SN1987A, Cooling of Sun and globular clusters, White dwarfs	$\gamma + \mu \rightarrow A' + \mu$, $\mu + p \rightarrow \mu + p + A'$, $\mu^+\mu^- \rightarrow A'$ at tree level, $e^+e^- \rightarrow A'$ through kinetic mixing.	$A' \rightarrow \eta\eta, \nu_s\nu_s$ (if decays to $\nu\nu, e^+e^-$ then can not escape), $\phi' \rightarrow \eta\eta, \nu\nu$	Stellar cooling rules out: $m_{A'}, m_{\phi'} \leq 1 \text{ MeV}$. WD constraint are negligible if $m_\eta, m_{\nu_s} \geq 0.1 \text{ MeV}$. (All these astrophysical bounds can be evaded using chameleon effect.)
Cosmological probes	ΔN_{eff} value	$\mu^+\mu^- \rightarrow \gamma A'$, production of longitudinal mode get enhanced due to axial vector coupling.	invisible states	If the Universe reheat at a temperature $\geq 100 \text{ MeV}$, $m_{A'}, m_{\phi'} \leq 1 \text{ MeV}$ is ruled out. (Can be evaded if reheat occurs at a lower temperature.)

Type of experiments	Name of the experiment	Production of A'/ϕ'	Final states	Results
Muon beam experiments	NA64 μ , LDMX-M ³ (nearby detectors)	μ -bremsstrahlung	Can probe when A'/ϕ' has a significant decay rate to invisible states such as $\nu\nu, \eta\eta$	NA64 μ , LDMX-M ³ can probe the entire parameter space if $m_{A',\phi'} > 2m_{\eta,\nu_s}$ with $\text{Br}(\text{invisible}) > 10^{-4}$, even if $A'/\phi' \rightarrow \mu^+\mu^-$ is allowed still $\text{Br}(\text{invisible}) > 10^{-4}$ provided $m_{\eta,\nu_s} > 1$ MeV. Can be probed by looking at nuclear/electron recoil.
Neutrino experiments	COHERENT, CCM JSNS ²	p/e - bremsstrahlung, meson decay	$A' \rightarrow \nu_s\nu_s/\eta\eta$, $\nu_s/\eta_i + N \rightarrow \nu_s/\eta_j + N$ generate nuclear recoil, $\nu_s/\eta_i + e \rightarrow \nu_s/\eta_j + e$ generate electron recoil	$m_{A'} \sim 30$ MeV can explain the $2.4\text{--}3\sigma$ excess found by COHERENT, $m_{A'} \gtrsim 30$ MeV is ruled out. CCM and JSNS ² will improve the sensitivity.

Acknowledgments We are grateful to Asher Berlin and Jeremy Sakstein for useful discussions. We acknowledge Shannon Kumar for her hospitality. The work of BD and SG are supported in part by the DOE Grant No. DE-SC0010813. The work of JK is supported in part by DOE Grant No. DE-SC0010504.

References

- [1] J. C. Pati and A. Salam, “Lepton Number as the Fourth Color,” *Phys. Rev.* **D10** (1974) 275–289. [Erratum: *Phys. Rev.* D11,703(1975)].
- [2] R. N. Mohapatra and J. C. Pati, “A Natural Left-Right Symmetry,” *Phys. Rev.* **D11** (1975) 2558.
- [3] G. Senjanovic and R. N. Mohapatra, “Exact Left-Right Symmetry and Spontaneous Violation of Parity,” *Phys. Rev.* **D12** (1975) 1502.
- [4] B. Dutta, S. Ghosh, and J. Kumar, “A sub-GeV dark matter model,” *Phys. Rev. D* **100** (2019) 075028, [arXiv:1905.02692 \[hep-ph\]](#).
- [5] B. Dutta, D. Kim, S. Liao, J.-C. Park, S. Shin, and L. E. Strigari, “Dark matter signals from timing spectra at neutrino experiments,” *Phys. Rev. Lett.* **124** no. 12, (2020) 121802, [arXiv:1906.10745 \[hep-ph\]](#).
- [6] B. Batell, A. Freitas, A. Ismail, and D. Mckeen, “Flavor-specific scalar mediators,” *Phys. Rev. D* **98** no. 5, (2018) 055026, [arXiv:1712.10022 \[hep-ph\]](#).
- [7] B. Dutta, S. Ghosh, and J. Kumar, “Contributions to ΔN_{eff} From the Dark Photon of $U(1)_{T3R}$,” *Phys. Rev. D* **102** no. 1, (2020) 015013, [arXiv:2002.01137 \[hep-ph\]](#).
- [8] R. Diener, S. Godfrey, and I. Turan, “Constraining Extra Neutral Gauge Bosons with Atomic Parity Violation Measurements,” *Phys. Rev. D* **86** (2012) 115017, [arXiv:1111.4566 \[hep-ph\]](#).
- [9] J. P. Leveille, “The Second Order Weak Correction to (G-2) of the Muon in Arbitrary Gauge Models,” *Nucl. Phys. B* **137** (1978) 63–76.
- [10] BaBar Collaboration, B. Aubert *et al.*, “Search for Dimuon Decays of a Light Scalar Boson in Radiative Transitions Upsilon $\rightarrow \gamma$ gamma A0,” *Phys. Rev. Lett.* **103** (2009) 081803, [arXiv:0905.4539 \[hep-ex\]](#).
- [11] BaBar Collaboration, J. Lees *et al.*, “Search for a Dark Photon in e^+e^- Collisions at BaBar,” *Phys. Rev. Lett.* **113** no. 20, (2014) 201801, [arXiv:1406.2980 \[hep-ex\]](#).
- [12] L. Landau, “On the angular momentum of a system of two photons,” *Dokl. Akad. Nauk SSSR* **60** no. 2, (1948) 207–209.
- [13] C.-N. Yang, “Selection Rules for the Dematerialization of a Particle Into Two Photons,” *Phys. Rev.* **77** (1950) 242–245.

- [14] R. Harnik, J. Kopp, and P. A. Machado, “Exploring ν Signals in Dark Matter Detectors,” *JCAP* **07** (2012) 026, [arXiv:1202.6073 \[hep-ph\]](#).
- [15] J. Redondo, “Helioscope Bounds on Hidden Sector Photons,” *JCAP* **07** (2008) 008, [arXiv:0801.1527 \[hep-ph\]](#).
- [16] R. Bollig, W. DeRocco, P. W. Graham, and H.-T. Janka, “Muons in supernovae: implications for the axion-muon coupling,” [arXiv:2005.07141 \[hep-ph\]](#).
- [17] D. Croon, G. Elor, R. K. Leane, and S. D. McDermott, “Supernova Muons: New Constraints on Z' Bosons, Axions, and ALPs,” [arXiv:2006.13942 \[hep-ph\]](#).
- [18] R. Foot, “New Physics From Electric Charge Quantization?,” *Mod. Phys. Lett.* **A6** (1991) 527–530.
- [19] X. G. He, G. C. Joshi, H. Lew, and R. R. Volkas, “NEW Z-prime PHENOMENOLOGY,” *Phys. Rev.* **D43** (1991) 22–24.
- [20] X.-G. He, G. C. Joshi, H. Lew, and R. R. Volkas, “Simplest Z-prime model,” *Phys. Rev.* **D44** (1991) 2118–2132.
- [21] D. Borah, L. Mukherjee, and S. Nandi, “Low Scale $U(1)_X$ Gauge Symmetry as an Origin of Dark Matter, Neutrino Mass and Flavour Anomalies,” [arXiv:2007.13778 \[hep-ph\]](#).
- [22] D. B. Costa, “Simple anomaly-free $U(1)$ extensions of the Standard Model,” [arXiv:2007.08733 \[hep-ph\]](#).
- [23] **Planck** Collaboration, N. Aghanim *et al.*, “Planck 2018 results. VI. Cosmological parameters,” [arXiv:1807.06209 \[astro-ph.CO\]](#).
- [24] H. K. Dreiner, J.-F. Fortin, J. Isern, and L. Ubaldi, “White Dwarfs constrain Dark Forces,” *Phys. Rev. D* **88** (2013) 043517, [arXiv:1303.7232 \[hep-ph\]](#).
- [25] A. E. Nelson and J. Walsh, “Short Baseline Neutrino Oscillations and a New Light Gauge Boson,” *Phys. Rev. D* **77** (2008) 033001, [arXiv:0711.1363 \[hep-ph\]](#).
- [26] B. Feldman and A. E. Nelson, “New regions for a chameleon to hide,” *JHEP* **08** (2006) 002, [arXiv:hep-ph/0603057](#).
- [27] A. Nelson and J. Walsh, “Chameleon vector bosons,” *Phys. Rev. D* **77** (2008) 095006, [arXiv:0802.0762 \[hep-ph\]](#).
- [28] M. Bauer, P. Foldenauer, and J. Jaeckel, “Hunting All the Hidden Photons,” *JHEP* **18** (2020) 094, [arXiv:1803.05466 \[hep-ph\]](#).
- [29] E. Riordan *et al.*, “A Search for Short Lived Axions in an Electron Beam Dump Experiment,” *Phys. Rev. Lett.* **59** (1987) 755.
- [30] J. Bjorken, S. Ecklund, W. Nelson, A. Abashian, C. Church, B. Lu, L. Mo, T. Nunamaker, and P. Rassmann, “Search for Neutral Metastable Penetrating Particles Produced in the SLAC Beam Dump,” *Phys. Rev. D* **38** (1988) 3375.
- [31] J. D. Bjorken, R. Essig, P. Schuster, and N. Toro, “New Fixed-Target Experiments to Search for Dark Gauge Forces,” *Phys. Rev. D* **80** (2009) 075018, [arXiv:0906.0580 \[hep-ph\]](#).
- [32] M. Davier and H. Nguyen Ngoc, “An Unambiguous Search for a Light Higgs Boson,” *Phys. Lett. B* **229** (1989) 150–155.
- [33] S. Gninenko, N. Krasnikov, and V. Matveev, “Muon $g-2$ and searches for a new leptophobic sub-GeV dark boson in a missing-energy experiment at CERN,” *Phys. Rev. D* **91** (2015) 095015, [arXiv:1412.1400 \[hep-ph\]](#).
- [34] M. Bordag, U. Mohideen, and V. Mostepanenko, “New developments in the Casimir effect,” *Phys. Rept.* **353** (2001) 1–205, [arXiv:quant-ph/0106045](#).
- [35] J. L. Feng, I. Galon, F. Kling, and S. Trojanowski, “ForwArd Search ExpeRiment at the LHC,” *Phys. Rev. D* **97** no. 3, (2018) 035001, [arXiv:1708.09389 \[hep-ph\]](#).
- [36] **FASER** Collaboration, A. Ariga *et al.*, “Letter of Intent for FASER: ForwArd Search ExpeRiment at the LHC,” [arXiv:1811.10243 \[physics.ins-det\]](#).

- [37] **FASER** Collaboration, A. Ariga *et al.*, “Technical Proposal for FASER: ForwArd Search ExpeRiment at the LHC,” [arXiv:1812.09139 \[physics.ins-det\]](#).
- [38] **FASER** Collaboration, A. Ariga *et al.*, “FASER’s physics reach for long-lived particles,” *Phys. Rev. D* **99** no. 9, (2019) 095011, [arXiv:1811.12522 \[hep-ph\]](#).
- [39] **FASER** Collaboration, A. Ariga *et al.*, “FASER: ForwArd Search ExpeRiment at the LHC,” [arXiv:1901.04468 \[hep-ex\]](#).
- [40] **SHiP** Collaboration, M. Anelli *et al.*, “A facility to Search for Hidden Particles (SHiP) at the CERN SPS,” [arXiv:1504.04956 \[physics.ins-det\]](#).
- [41] S. Alekhin *et al.*, “A facility to Search for Hidden Particles at the CERN SPS: the SHiP physics case,” *Rept. Prog. Phys.* **79** no. 12, (2016) 124201, [arXiv:1504.04855 \[hep-ph\]](#).
- [42] **LDMX** Collaboration, J. Mans, “The LDMX Experiment,” *EPJ Web Conf.* **142** (2017) 01020.
- [43] **LDMX** Collaboration, T. Åkesson *et al.*, “Light Dark Matter eXperiment (LDMX),” [arXiv:1808.05219 \[hep-ex\]](#).
- [44] **LDMX** Collaboration, O. Moreno, “The Light Dark Matter eXperiment (LDMX),” *PoS ICHEP2018* (2019) 395.
- [45] **LDMX** Collaboration, T. Åkesson *et al.*, “A High Efficiency Photon Veto for the Light Dark Matter eXperiment,” *JHEP* **04** (2020) 003, [arXiv:1912.05535 \[physics.ins-det\]](#).
- [46] A. Berlin, N. Blinov, G. Krnjaic, P. Schuster, and N. Toro, “Dark Matter, Millicharges, Axion and Scalar Particles, Gauge Bosons, and Other New Physics with LDMX,” *Phys. Rev. D* **99** no. 7, (2019) 075001, [arXiv:1807.01730 \[hep-ph\]](#).
- [47] A. Berlin, S. Gori, P. Schuster, and N. Toro, “Dark Sectors at the Fermilab SeaQuest Experiment,” *Phys. Rev. D* **98** no. 3, (2018) 035011, [arXiv:1804.00661 \[hep-ph\]](#).
- [48] **SeaQuest** Collaboration, C. Aidala *et al.*, “The SeaQuest Spectrometer at Fermilab,” *Nucl. Instrum. Meth. A* **930** (2019) 49–63, [arXiv:1706.09990 \[physics.ins-det\]](#).
- [49] **COHERENT** Collaboration, D. Akimov *et al.*, “Observation of Coherent Elastic Neutrino-Nucleus Scattering,” *Science* **357** no. 6356, (2017) 1123–1126, [arXiv:1708.01294 \[nucl-ex\]](#).
- [50] **COHERENT** Collaboration, D. Akimov *et al.*, “COHERENT Collaboration data release from the first observation of coherent elastic neutrino-nucleus scattering,” [arXiv:1804.09459 \[nucl-ex\]](#).
- [51] **COHERENT** Collaboration, D. Akimov *et al.*, “COHERENT 2018 at the Spallation Neutron Source,” [arXiv:1803.09183 \[physics.ins-det\]](#).
- [52] **COHERENT** Collaboration, D. Akimov *et al.*, “Sensitivity of the COHERENT Experiment to Accelerator-Produced Dark Matter,” [arXiv:1911.06422 \[hep-ex\]](#).
- [53] **COHERENT** Collaboration, D. Akimov *et al.*, “First Detection of Coherent Elastic Neutrino-Nucleus Scattering on Argon,” [arXiv:2003.10630 \[nucl-ex\]](#).
- [54] **Crystal Barrel** Collaboration, C. Amsler *et al.*, “Search for a new light gauge boson in decays of π^0 and η ,” *Phys. Lett. B* **333** (1994) 271–276.
- [55] **Crystal Barrel** Collaboration, C. Amsler *et al.*, “Search for a new light gauge boson in π^0 , η and η' -prime decays,” *Z. Phys. C* **70** (1996) 219–226.
- [56] C.-Y. Chen, M. Pospelov, and Y.-M. Zhong, “Muon Beam Experiments to Probe the Dark Sector,” *Phys. Rev. D* **95** no. 11, (2017) 115005, [arXiv:1701.07437 \[hep-ph\]](#).
- [57] S. Gninenko, D. Kirpichnikov, M. Kirsanov, and N. Krasnikov, “Combined search for light dark matter with electron and muon beams at NA64,” *Phys. Lett. B* **796** (2019) 117–122, [arXiv:1903.07899 \[hep-ph\]](#).
- [58] Y. Kahn, G. Krnjaic, N. Tran, and A. Whitbeck, “ M^3 : a new muon missing momentum experiment to probe $(g - 2)$ and dark matter at Fermilab,” *JHEP* **09** (2018) 153, [arXiv:1804.03144 \[hep-ph\]](#).
- [59] **Belle-II** Collaboration, T. Abe *et al.*, “Belle II Technical Design Report,” [arXiv:1011.0352 \[physics.ins-det\]](#).

- [60] G. Inguglia, “Belle II studies of missing energy decays and searches for dark photon production,” *PoS DIS2016* (2016) 263, [arXiv:1607.02089 \[hep-ex\]](#).
- [61] A. A. Aguilar-Arevalo *et al.*, *Fundamental Neutrino Physics at the Lujan Center*, March, 2018. "https://p25ext.lanl.gov/~lee/CaptainMills/Documentation/CCM_Proposal_Lujan_2018_V1.pdf".
- [62] E. Dunton, *Searching for Sterile Neutrinos with Coherent Captain Mills*, November, 2019. "<https://zenodo.org/record/3597486#.XyC-yi05RaE>". gnificent CEvNS 201.
- [63] **JSNS2** Collaboration, M. Harada *et al.*, “Proposal: A Search for Sterile Neutrino at J-PARC Materials and Life Science Experimental Facility,” [arXiv:1310.1437 \[physics.ins-det\]](#).
- [64] S. Ajimura *et al.*, “On-site background measurements for the J-PARC E56 experiment: A search for the sterile neutrino at J-PARC MLF,” *PTEP* **2015** no. 6, (2015) 063C01, [arXiv:1502.06324 \[physics.ins-det\]](#).
- [65] **JSNS2** Collaboration, M. Harada *et al.*, “Status Report for the 20th J-PARC PAC : A Search for Sterile Neutrino at J-PARC MLF (J-PARC E56, JSNS2),” [arXiv:1507.07076 \[physics.ins-det\]](#).
- [66] S. Ajimura *et al.*, “Technical Design Report (TDR): Searching for a Sterile Neutrino at J-PARC MLF (E56, JSNS2),” [arXiv:1705.08629 \[physics.ins-det\]](#).
- [67] **JSNS2** Collaboration, C. Rott, “Status of JSNS² - J-PARC Sterile Neutrino Search at J-PARC Spallation Neutron Source,” *J. Phys. Conf. Ser.* **1468** no. 1, (2020) 012176.
- [68] D. Z. Freedman, “Coherent Neutrino Nucleus Scattering as a Probe of the Weak Neutral Current,” *Phys. Rev. D* **9** (1974) 1389–1392.
- [69] V. Kopeliovich and L. Frankfurt, “Isotopic and chiral structure of neutral current,” *JETP Lett.* **19** (1974) 145–147.
- [70] B. Dutta, D. Kim, S. Liao, J.-C. Park, S. Shin, L. E. Strigari, and A. Thompson, “Searching for Dark Matter Signals in Timing Spectra at Neutrino Experiments,” [arXiv:2006.09386 \[hep-ph\]](#).
- [71] P. deNiverville, M. Pospelov, and A. Ritz, “Observing a light dark matter beam with neutrino experiments,” *Phys. Rev. D* **84** (2011) 075020, [arXiv:1107.4580 \[hep-ph\]](#).
- [72] **MiniBooNE DM** Collaboration, A. A. Aguilar-Arevalo, “Search for Dark Matter in the beam-dump of a proton beam with MiniBooNE,” *J. Phys. Conf. Ser.* **912** no. 1, (2017) 012017.
- [73] **MiniBooNE DM** Collaboration, A. Aguilar-Arevalo *et al.*, “Dark Matter Search in Nucleon, Pion, and Electron Channels from a Proton Beam Dump with MiniBooNE,” *Phys. Rev. D* **98** no. 11, (2018) 112004, [arXiv:1807.06137 \[hep-ex\]](#).
- [74] **MiniBooNE DM** Collaboration, A. A. Aguilar-Arevalo, “MiniBooNE-DM: a dark matter search in a proton beam dump,” *J. Phys. Conf. Ser.* **1342** no. 1, (2020) 012055, [arXiv:1907.04901 \[hep-ex\]](#).
- [75] **LSND** Collaboration, L. Auerbach *et al.*, “Measurement of electron - neutrino - electron elastic scattering,” *Phys. Rev. D* **63** (2001) 112001, [arXiv:hep-ex/0101039](#).
- [76] **LSND** Collaboration, A. Aguilar-Arevalo *et al.*, “Evidence for neutrino oscillations from the observation of $\bar{\nu}_e$ appearance in a $\bar{\nu}_\mu$ beam,” *Phys. Rev. D* **64** (2001) 112007, [arXiv:hep-ex/0104049](#).
- [77] **DUNE** Collaboration, J. Strait, “DUNE Physics,” in *17th International Workshop on Neutrino Factories and Future Neutrino Facilities*. 8, 2015.
- [78] **DUNE** Collaboration, A. Habig, “An Experimental Program in Neutrinos, Nucleon Decay and Astroparticle Physics Enabled by the Fermilab Long-Baseline Neutrino Facility,” *PoS EPS-HEP2015* (2015) 041.
- [79] **DUNE** Collaboration, B. Abi *et al.*, “Deep Underground Neutrino Experiment (DUNE), Far Detector Technical Design Report, Volume I Introduction to DUNE,” [arXiv:2002.02967 \[physics.ins-det\]](#).
- [80] **DUNE** Collaboration, B. Abi *et al.*, “Deep Underground Neutrino Experiment (DUNE), Far Detector Technical Design Report, Volume II DUNE Physics,” [arXiv:2002.03005 \[hep-ex\]](#).
- [81] **DUNE** Collaboration, B. Abi *et al.*, “Deep Underground Neutrino Experiment (DUNE), Far Detector Technical Design Report, Volume III DUNE Far Detector Technical Coordination,” [arXiv:2002.03008 \[physics.ins-det\]](#).

- [82] **DUNE** Collaboration, B. Abi *et al.*, “Deep Underground Neutrino Experiment (DUNE), Far Detector Technical Design Report, Volume IV Far Detector Single-phase Technology,” [arXiv:2002.03010 \[physics.ins-det\]](#).
- [83] C. Giunti, “General COHERENT constraints on neutrino nonstandard interactions,” *Phys. Rev. D* **101** no. 3, (2020) 035039, [arXiv:1909.00466 \[hep-ph\]](#).
- [84] M. Gonzalez-Garcia and M. Maltoni, “Determination of matter potential from global analysis of neutrino oscillation data,” *JHEP* **09** (2013) 152, [arXiv:1307.3092 \[hep-ph\]](#).
- [85] I. Esteban, M. Gonzalez-Garcia, M. Maltoni, I. Martinez-Soler, and J. Salvado, “Updated Constraints on Non-Standard Interactions from Global Analysis of Oscillation Data,” *JHEP* **08** (2018) 180, [arXiv:1805.04530 \[hep-ph\]](#).
- [86] I. Esteban, M. Gonzalez-Garcia, and M. Maltoni, “On the Determination of Leptonic CP Violation and Neutrino Mass Ordering in Presence of Non-Standard Interactions: Present Status,” *JHEP* **06** (2019) 055, [arXiv:1905.05203 \[hep-ph\]](#).
- [87] B. Dutta, R. F. Lang, S. Liao, S. Sinha, L. Strigari, and A. Thompson, “A global analysis strategy to resolve neutrino NSI degeneracies with scattering and oscillation data,” [arXiv:2002.03066 \[hep-ph\]](#).
- [88] **Hyper-Kamiokande Proto** Collaboration, J. Migenda, “The Hyper-Kamiokande Experiment: Overview & Status,” in *Prospects in Neutrino Physics*. 4, 2017. [arXiv:1704.05933 \[hep-ex\]](#).
- [89] **Hyper-Kamiokande Proto** Collaboration, M. Yokoyama, “The Hyper-Kamiokande Experiment,” in *Prospects in Neutrino Physics*. 4, 2017. [arXiv:1705.00306 \[hep-ex\]](#).
- [90] **Hyper-Kamiokande proto** Collaboration, M. Jiang, “Sensitivity of new physics by joint analysis of neutrino oscillation on Hyper-Kamiokande,” *J. Phys. Conf. Ser.* **888** no. 1, (2017) 012111.
- [91] **Hyper-Kamiokande proto** Collaboration, C. Bronner, “Physics potential of Hyper-Kamiokande for neutrino oscillation measurements,” *PoS NuFact2017* (2018) 053.
- [92] **Hyper-Kamiokande Proto** Collaboration, T. Yano, “Astroparticle Physics in Hyper-Kamiokande,” *J. Phys. Conf. Ser.* **1468** no. 1, (2020) 012146.
- [93] **Hyper-Kamiokande Proto-** Collaboration, Y. Kudenko, “Hyper-Kamiokande,” in *International Conference on Instrumentation for Colliding Beam Physics*. 5, 2020. [arXiv:2005.13641 \[physics.ins-det\]](#).
- [94] P. F. Smith, “Proposed experiments to detect keV range sterile neutrinos using energy-momentum reconstruction of beta decay or K-capture events,” *New J. Phys.* **21** no. 5, (2019) 053022, [arXiv:1607.06876 \[physics.ins-det\]](#).
- [95] **KATRIN** Collaboration, S. Mertens *et al.*, “A novel detector system for KATRIN to search for keV-scale sterile neutrinos,” *J. Phys. G* **46** no. 6, (2019) 065203, [arXiv:1810.06711 \[physics.ins-det\]](#).